8th IFAC Symposium on Advanced Control of Chemical Processes
The International Federation of Automatic Control
Singapore, July 10-13, 2012

Model reduction of a batch drum granulator by proper orthogonal decomposition

Michael Mangold *

* *Max Planck Institute for Dynamics of Complex Technical Systems, Sandtorstr. 1, 39106 Magdeburg, Germany (Tel: +49-391-6110361; e-mail: mangold@mpi-magdeburg.mpg.de).*

Abstract: Particle processes with agglomeration or breakage are often described by population balances. This leads to mathematical models containing partial integro differential equations. It is quite challenging to solve such equations numerically and to apply them to process control tasks. Reduced models for agglomeration and breakage processes are desirable. In this contribution, the use of proper orthogonal decomposition is suggested as a method to derive such reduced models. The reduction method is applied to a batch granulator. A low order model is formulated and found to be in good agreement with the reference model. The usefulness of the low order model is demonstrated by applying it to an optimal control problem.

Keywords: particulate processing; distributed parameter systems; nonlinear systems; model reduction; optimal control; population balance system; proper orthogonal decomposition; granulation

1. INTRODUCTION

Particle processes play an important role in chemical and pharmaceutical industry. Crystallization, granulation or polymerization and prominent examples for this class of processes. Population balance equations have been widely accepted as an appropriate tool to describe particle processes mathematically [Ramkrishna, 2000]. Population balances typically are partial differential equations, whose independent variables are the time and one or several characteristic particle properties like the characteristic particle size or the particle composition.

An important difference between population balance systems and spatially distributed systems is that the interaction between two points in space usually decreases with their distance, whereas in population balances strong interactions may occur between remote points on the property coordinate. Examples are breakage phenomena, where a larger particle breaks into several smaller ones, or agglomeration phenomena, where two small particles merge to a larger one. Agglomeration and breakage cause integral terms in the population balances and turn the population balances into partial integro differential equations. The numerical treatment of this type of equations is quite challenging. Further, the complicated structure of the equations makes it to hard to apply them to the solution of process control problems as it limits the number of applicable controller design techniques. In literature, nonlinear model predictive control has been suggested by several authors to overcome this problem, e.g. [Glaser et al., 2009]. It would be desirable to simplify the process model of agglomeration processes in such a way that a broader class of control algorithms becomes applicable.

The method of moments and its extensions are frequently used to reduce population balance equations to low order model systems [Marchisio et al., 2003]. Although well developed, it may be seen as a certain drawback of the method that the resulting reduced model only describes the moments of a particle distribution, but not the distribution itself.

An alternative model reduction approach consists in the use of proper orthogonal decomposition (POD) methods. The key idea is to approximate the property distributions by a linear combination of problem specific basis functions, which are computed from solutions of the detailed reference model. The method requires test simulations with the detailed model to generate the basis functions and further coefficients of the reduced model. This preparation step may be computationally quite expensive, but as a reward one obtains a nonlinear reduced model of low order that can be solved quite easily.

In previous publications, proper orthogonal decomposition could be applied successfully to the model reduction of a crystallization process with particle growth and complex fluid dynamics [Krasnyk et al., 2012]. The objective of this work is to show that the method is also well suited to treat agglomeration processes, because it generates reduced models with a nice and simple structure.

A drum granulator model from literature is used to illustrate the model reduction method. The reference model is briefly introduced in Section 2. Section 3 contains the main part of the work. It discusses the model reduction procedure and compares the reduced model with the reference model. Section 4 finally presents a strategy to solve an optimal control problem based on the reduced model.

2. REFERENCE MODEL

Granulation is a technique used to enlarge particles by mixing them with a liquid, the binder, that agglomerates smaller particles to larger units. Granulation is often done in rotating drums containing the solid. In batch operation, a powder of fine particles is filled into the drum at the beginning of the process. During the process, liquid binder is added at a certain defined spray rate. How to change the binder spray rate over time in order to get particles with desired properties is a major design problem for this type of process.

The following work is based on a dynamic model of a drum granulator published by Wang et al. [2006]. In the variant used here, the model assumes perfect mixing inside the drum, i.e. it is space independent. The particle mass density distributions are described as a function of the time and a characteristic particle size. The main physical phenomena accounted for are particle growth and particle agglomeration. The model consists of a population balance for the solid particle, a balance for the powder mass, and a balance for the liquid content of the drum. The balance equations are listed in the following.

- The population balance for the particle mass density distribution $m(L,t)$, where L is the characteristic particle size, reads:

$$\frac{\partial m}{\partial t} = -L^3 \frac{\partial}{\partial L}\left(G\frac{m}{L^3}\right) + \frac{L^5}{2}\int_{L_{min}}^{L} \frac{6}{\pi\rho}\frac{\beta\left(\left(L^3-\lambda^3\right)^{\frac{1}{3}},\lambda\right)}{\left(L^3-\lambda^3\right)^{\frac{2}{3}}} \frac{m\left(\left(L^3-\lambda^3\right)^{\frac{1}{3}},t\right)}{L^3-\lambda^3}\frac{m(\lambda),t}{\lambda^3}d\lambda - m(L,t)\frac{6}{\pi\rho}\int_{L_{min}}^{L_{max}} \beta(L,\lambda)\frac{m(\lambda,t)}{\lambda^3}d\lambda \quad (1)$$

  The first term on the right hand side of (1) describes particle growth with a growth rate G, which is size independent and a function of the powder mass and the liquid content. The second and the third term describe changes in the particle mass distribution due to agglomeration; β is the coalescence kernel given by

$$\beta = \beta_0(x_w)\frac{(L+\lambda)^2}{L\,\lambda} \quad (2)$$

  For the precise definition of G and β_0 see [Wang et al., 2006].
- The particle growth causes a mass transfer from the fine powder to the particle phase. The balance for the fine powder mass M_{powder} reads

$$\frac{dM_{powder}}{dt} = \int_{L_{min}}^{L_{max}} L^3 \frac{\partial}{\partial L}\left(G\frac{m}{L^3}\right)dL \quad (3)$$

- A differential equation for the liquid content x_w follows from the liquid mass balance:

$$M_{total}\frac{dx_w}{dt} = R_w \quad (4)$$

  In (4) $M_{total} = \int_{L_{min}}^{L_{max}} m(L,t)dL + M_{powder}$ is the total solid mass, and R_w is the binder spray rate.

To solve the reference equations numerically, the mass conserving discretization scheme by Litster et al. [1995] with $i_{max} = 20$ size intervals and $q = 4$ internal discretizations per size interval is used.

3. MODEL REDUCTION

The technique of proper orthogonal decomposition (POD) [Sirovich, 1987, Park and Cho, 1996, Kunisch and Volkwein, 2003] is applied to obtain a reduced model. As a first step, the particle mass density function is expressed by the series approach

$$m(L,t) \approx \sum_{i=1}^{N} \mu_i(t)\psi_i(L) \quad (5)$$

The space dependent basis functions $\psi_i(L)$ are computed from test simulations with the reference model. Differential equations for the time dependent functions $\mu_i(t)$ are obtained from Galerkin's method of weighted residuals. Both steps are explained in the following.

3.1 Generation of basis functions

Proper orthogonal decomposition uses problem specific basis functions. A set of orthonormal basis functions is generated from test simulations with the reference model, so-called snapshots. In the drum granulator example, the snapshots are dynamic solutions of the particle mass density distribution $m(L,t)$ at N_s time points $t_1,\ldots,t_{N_s}$. The basis functions are chosen in such a way that they approximate the average of the snapshots in a best possible way. This can be formulated as the optimization problem for a basis function $\psi_j(L)$:

$$\sum_{s=1}^{N_s}\big(m(L,t_s) - (m(L,t_s),\psi_j(L))_\Omega\,\psi_j(L), \; m(L,t_s) - (m(L,t_s),\psi_j(L))_\Omega\,\psi_j(L)\big)_\Omega \stackrel{!}{=} \min \quad (6)$$

The brackets $(.,.)_\Omega$ denote the scalar product:

$$(f(L),g(L))_\Omega = \int_{L_{min}}^{L_{max}} f(L)\;g(L)\;dL \quad (7)$$

The term $(m(L,t_s),\psi_j(L))_\Omega = \mu_j(t_s)$ is the projection of the snapshot $m(L,t_s)$ on $\psi_j(L)$. The optimization problem (6) is constrained by the scaling condition

$$(\psi_j(L),\psi_j(L))_\Omega = 1 \quad (8)$$

When expressing the basis functions by

$$\psi_j(L) = \sum_{s=1}^{N_s} m(L,t_s)\;v_{sj} \quad (9)$$

with still unknown coefficients v_{sj}, it can be shown that the optimization problem (6, 8) may be transformed into the eigenvalue problem

$$\underbrace{\begin{pmatrix} M_{11} & M_{12} & \cdots & M_{1N_s} \\ M_{21} & M_{22} & \cdots & M_{2N_s} \\ \vdots & \ddots & & \vdots \\ M_{N_s1} & M_{N_s2} & \cdots & M_{N_sN_s} \end{pmatrix}}_{=:\boldsymbol{M}} \underbrace{\begin{pmatrix} v_{1j} \\ v_{2j} \\ \vdots \\ v_{N_sj} \end{pmatrix}}_{=:\boldsymbol{v}_j} = \lambda_j \begin{pmatrix} v_{1j} \\ v_{2j} \\ \vdots \\ v_{N_sj} \end{pmatrix} \quad (10)$$

where M_{ij} is the abbreviation for the scalar product of two snapshots:

$$M_{ij} = (m(L,t_i), m(L,t_j))_\Omega \quad (11)$$

As $\boldsymbol{M}$ is symmetric, the eigenvectors $\boldsymbol{v}_j$ are orthogonal. It is easy to show that therefore the basis functions are orthogonal, as well, i.e.

$$(\psi_j(L), \psi_k(L))_\Omega = 0 \text{ for } j \neq k \quad (12)$$

The eigenvalues λ_j may be interpreted as a measure for how relevant the basis function ψ_j is for the reproduction of the snapshots [Holmes et al., 1998]. A small value of λ_j means that the corresponding basis function does not contribute significantly to the approximation of the snapshots and may be neglected. In this sense the eigenvalues of $\boldsymbol{M}$ help to choose an appropriate number N of basis functions in the series approximation (5) for $m(L,t)$.

In summary, the computation of basis functions requires (i) the generation of N_s snapshots, (ii) the generation of the $N_s \times N_s$ matrix $\boldsymbol{M}$ and (iii) the solution of the eigenvalue problem (10). Especially the first step may computationally expensive if the reference model is complex. However, one should note that the computation time needed to generate the basis functions does not increase the computation time for the solution of the reduced model, as the basis functions are generated before solving the reduced model.

For illustration, Figure 1 shows the first three basis functions of the drum granulator problem.

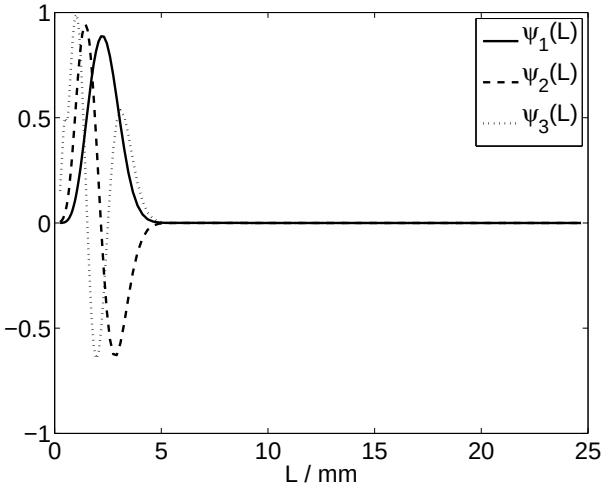

Fig. 1. First three basis functions of the reduced drum granulator model

3.2 Derivation of reduced model equations

In order to obtain differential equations for the time dependent functions $\mu_j(t)$ in the series expression (5), the method of weighted residuals is applied. It is requested that, when inserting the approximation (5) for $m(L,t)$ into the population balance (1), the projection of the residual on the basis functions should vanish, i.e.

$$\begin{aligned}
\left(\frac{\partial m}{\partial t}, \psi_j\right)_\Omega &= -\left(L^3 \frac{\partial}{\partial L}\left(G\frac{m}{L^3}\right), \psi_j\right)_\Omega \\
&+ \left(\frac{L^5}{2} \int_{L_{min}}^{L} \frac{6}{\pi\rho} \frac{\beta\left(\left(L^3-\lambda^3\right)^{\frac{1}{3}}, \lambda\right)}{\left(L^3-\lambda^3\right)^{\frac{2}{3}}} \right. \\
&\qquad \left. \frac{m\left(\left(L^3-\lambda^3\right)^{\frac{1}{3}}, t\right)}{L^3-\lambda^3} \frac{m(\lambda),t}{\lambda^3} d\lambda,\ \psi_j \right)_\Omega \\
&- \left(m(L,t)\frac{6}{\pi\rho} \int_{L_{min}}^{L_{max}} \beta(L,\lambda)\frac{m(\lambda,t)}{\lambda^3} d\lambda,\ \psi_j\right)_\Omega \\
&\qquad\qquad (j = 1, \ldots, N) \quad (13)
\end{aligned}$$

The terms in (13) may be rearranged in the following way:

$$\left(\frac{\partial m}{\partial t}, \psi_j\right)_\Omega = \frac{d\mu_j}{dt} \quad (14)$$

$$\left(L^3 \frac{\partial}{\partial L}\left(G\frac{m}{L^3}\right), \psi_j\right)_\Omega = \quad (15)$$

$$G \sum_{i=1}^{N} \mu_i \underbrace{\left(L^3 \frac{\partial}{\partial L}\left(\frac{\psi_i}{L^3}\right), \psi_j\right)_\Omega}_{=:\, A_{ji}} \quad (16)$$

$$\begin{aligned}
&\left(\frac{L^5}{2} \int_{L_{min}}^{L} \frac{6}{\pi\rho} \frac{\beta\left(\left(L^3-\lambda^3\right)^{\frac{1}{3}}, \lambda\right)}{\left(L^3-\lambda^3\right)^{\frac{2}{3}}} \right. \\
&\qquad \left. \frac{m\left(\left(L^3-\lambda^3\right)^{\frac{1}{3}}, t\right)}{L^3-\lambda^3} \frac{m(\lambda),t}{\lambda^3} d\lambda,\ \psi_j \right)_\Omega \\
&= \sum_{i=1}^{N}\sum_{k=1}^{N} \frac{6}{\pi\rho}\, \beta_0(x_w)\, \mu_i(t)\, \mu_k(t) \\
&\underbrace{\int_{L=L_{min}}^{L_{max}} \int_{\lambda=L_{min}}^{L} \frac{L^5}{2\left(L^3-\lambda^3\right)^{\frac{2}{3}}} \frac{\left(\left(L^3-\lambda^3\right)^{\frac{1}{3}}+\lambda\right)^2}{\left(L^3-\lambda^3\right)^{\frac{4}{3}}\lambda^4} \right.} \\
&\qquad \left. \psi_i\left(\left(L^3-\lambda^3\right)^{\frac{1}{3}}\right) \psi_k(\lambda)\, d\lambda\, \psi_j(L)\, dL \right. \quad (17) \\
&\qquad\qquad =: B'_{jki} \\
&\left(m(L,t)\frac{6}{\pi\rho} \int_{L_{min}}^{L_{max}} \beta(L,\lambda)\frac{m(\lambda,t)}{\lambda^3} d\lambda,\ \psi_j\right)_\Omega \\
&= \sum_{i=1}^{N}\sum_{k=1}^{N} \frac{6}{\pi\rho}\, \beta_0(x_w)\, \mu_i(t)\, \mu_k(t)
\end{aligned}$$

$$\underbrace{\int_{L=L_{min}}^{L_{max}} \psi_i(L)\,\psi_j(L) \int_{\lambda=L_{min}}^{L_{max}} \frac{(L+\lambda)^2}{L\,\lambda^4}\psi_k(\lambda)\,d\lambda\,dL}_{=:\,B''_{jki}} \tag{18}$$

Inserting the approximation (5) for $m(L,t)$ into the powder mass balance (3) gives

$$\frac{dM_{powder}}{dt} = G\sum_{i=1}^{N}\mu_i(t)\underbrace{\int_{L_{min}}^{L_{max}} L^3\,\frac{\partial}{\partial L}\left(\frac{\psi_i}{L^3}\right)}_{=:\,C_i} \tag{19}$$

The coefficients A_{ji}, B'_{jki}, B''_{jki} and C_i have to be computed by numerical quadrature, which may be quite expensive. However, as the integrals depend only on the basis functions, the quadratures can be done offline, before the runtime of the reduced model. Therefore, their computation does not slow down the solution of the reduced model. For the reduced model, A_{ji}, B'_{jki}, B''_{jki} and C_i are just constant parameters.

3.3 Solution of the reduced model

During runtime of the reduced model, the following set of ordinary differential equations has to be solved ($j = 1,\ldots,N$):

$$\frac{d\mu_j}{dt} = -G\sum_{i=1}^{N} A_{ji}\,\mu_i + \frac{6}{\pi\rho}\,\beta_0(x_w)\sum_{i=1}^{N}\sum_{k=1}^{N}(B'_{jki}-B''_{jki})\,\mu_i\,\mu_k \tag{20}$$

$$\frac{dM_{powder}}{dt} = G\sum_{i=1}^{N} C_i\,\mu_i \tag{21}$$

$$M_{total}\frac{dx_w}{dt} = R_w \tag{22}$$

One can see that the reduced model system has a nice and simple structure with a sum of quadratic terms that replaces the integrals appearing in the original population balance (1). It is found that $N = 6$ basis functions approximate the particle mass density distribution sufficiently well, so the reduced model consists of eight differential equations.

A test simulation compares the reduced model and the reference. In the test, binder is added for the first 33 s (see Figure 2). Figure 3 shows the resulting size distributions. There is a good agreement between the reduced model and the reference solution. The objective of Section 4 will be to produce particles of a defined characteristic size. The range of desired particle sizes is indicated by the shaded area in Figure 3. Figure 4 shows the time evolution of the total mass of particles in the desired size range. Slightly negative values in the solution of the reduced model are caused by the partly negative basis functions. Obviously, the reduced model can only be an approximation of the original model, but is sufficiently close to the reference for

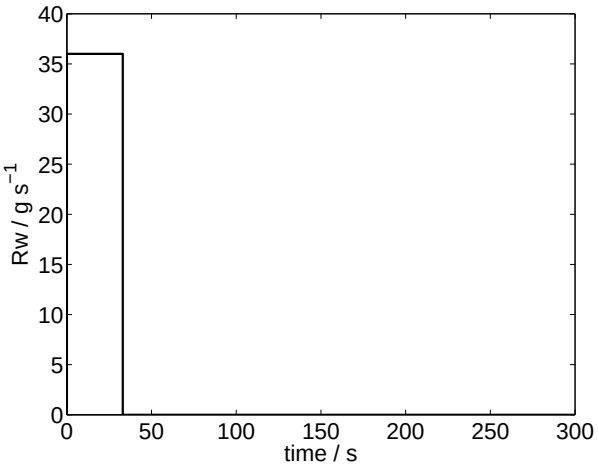

Fig. 2. Test scenario: Binder is added for the first 33 s with a constant rate, then the binder spray rate is set to zero.

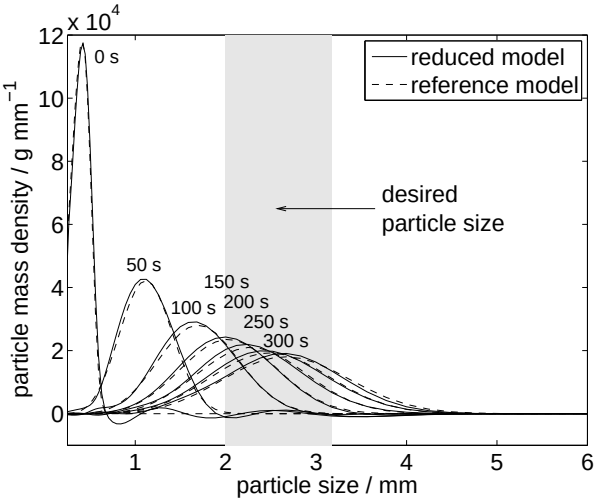

Fig. 3. Mass density distributions resulting from the binder spray rate in Figure 2

many applications. Figure 4 also shows the result, when the simpler discretization scheme by Hounslow et al. [1988] with 20 size intervals is used, as was done in the original paper by Wang et al. [2006], instead of the scheme by Litster et al. [1995] with 80 size intervals. Although the reduced POD model presented here is of lower order than the discretized model with 20 size intervals, its result is closer to the reference solution.

In literature, it has been seen as a drawback of spectral methods like the POD method applied here that these methods are not mass conservative [Bück et al., 2011]. In principle, this is true. However, in contrast to non-mass-conservative discretisation schemes, the variation of the total mass in this case is not a numerical inaccuracy, but lies in the nature of the projection method. This is illustrated by Figure 5, which shows the total mass of the particles when projected on the subspace defined by the basis functions. Although the total mass is constant in the reference simulation due to the mass conservative discretization scheme, the *projected* total mass in the reference simulation varies with time. This variation is re-

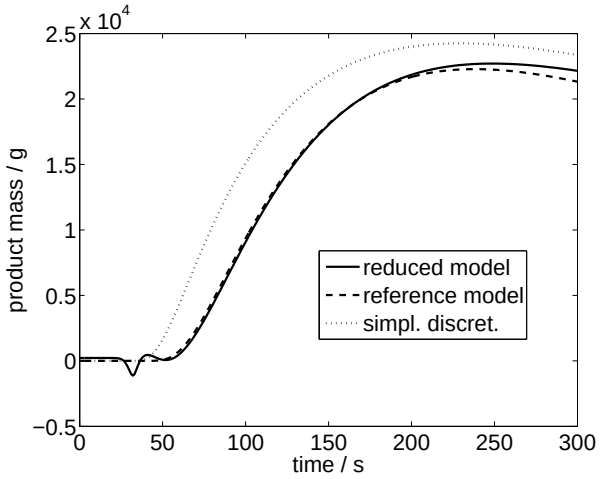

Fig. 4. Time evolution of the product mass; the dotted line is the numerical result, if the discretisation scheme by Hounslow et al. [1988] with 20 size intervals is used to solve the reference model.

produced by the reduced model with quite good accuracy.

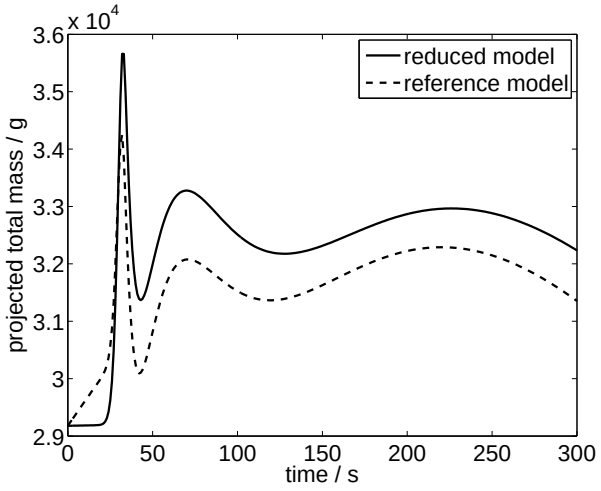

Fig. 5. Total mass of the particle distribution, when projected

In conclusion, the reduced model seems to describe the drum granulation process with sufficient accuracy to be applicable to control problems. This is studied in the next section.

4. OPTIMAL CONTROL

An optimal control problem for the batch drum granulator is considered that was stated by Wang et al. [2006]. The task is to produce as many particles as possible of the desired size range indicated in Figure 3, to do this as fast as possible, while minimizing the amount of binder fed during the batch process. Further, one has to obey the constraints that there is a maximum binder spray rate, that the binder spray rate must not become negative and that the spray rate can only change with a finite velocity. This task can be formulated as the following dynamic optimization problem:

$$\underset{R_w(t),\,t_f}{\text{minimize}} \left\{ -w_1\, M_{product}(t_f) + w_2 \int_0^{t_f} R_w(\theta)\, d\theta + w_3\, t_f \right\} \tag{23}$$

subject to

$$0 < R_w < R_{w,max}, \quad -\dot{R}_{w,max} < \dot{R}_w < \dot{R}_{max}$$
$$\text{model equations (1)-(4)} \tag{24}$$

In (23), t_f is the final time of the batch process, $M_{product}$ is the total mass of the particles with the desired size, and w_{1-3} are constant weighting coefficients. From the liquid mass balance, it is obvious that the integral $\int_0^{t_f} R_w(\theta)\, d\theta$ in the objective function (23) may also be written as $M_{total}\,(x_w(t_f) - x_w(0))$.

To solve the optimization problem, it is first observed that the particle growth rate G is rather small for the studied process and can be set to zero without a significant loss of accuracy. Therefore, when solving the optimization problem the particle growth is neglected. This has the big advantage that the equations for μ_j can be decoupled from x_w by the time scaling

$$\frac{d\tau}{dt} = 10^8\, \beta_0(x_w) \tag{25}$$

(The factor 10^8 is introduced only to obtain "nicer" values for τ). The differential equations for μ_j read in the scaled time:

$$\frac{d\mu_j}{d\tau} = \frac{6 \cdot 10^{-8}}{\pi\rho} \sum_{i=1}^{N} \sum_{k=1}^{N} (B'_{jki} - B''_{jki}) \mu_i\, \mu_k,\ j = 1, \ldots, N \tag{26}$$

and the product mass follows from

$$M_{product}(\tau) = \sum_{i=1}^{N} \mu_i(\tau) \sum_{L_{p,min}}^{L_{p,max}} \psi_i(L)\, dL, \tag{27}$$

where $L_{p,min}$ and $L_{p,max}$ are the minimum and maximum size, respectively, of particles in the product range. The nice thing about Equation (26) and (27) is that they do not have to be solved simultaneously with the solution of the optimization problem. As the equations are independent of R_w, $M_{product}(\tau)$ can be computed offline, and its value can be read from a look-up table during optimization.

To solve the remaining model equations, the scaled time τ serves as an parameterizing output of the system. It is expressed as a polynomial in t:

$$\tau = \sum_{i=1}^{n_p} a_i \left(\frac{t}{t_f} \right)^i \tag{28}$$

with free coefficients $a_1, \ldots, a_{n_p}$, which will become the optimization variables in the final formulation of the optimization problem (a_0 is set to zero in order to have $\tau = 0$ for $t = 0$). By differentiating (28) with respect to t and substituting $d\tau/dt$ with the right-hand side of (25) one obtains an implicit equation for x_w as a function of $a_1, \ldots, a_{n_p}, t_f, t$:

$$\beta_0(x_w) = 10^{-8} \sum_{i=1}^{n_p} \frac{a_i}{t_f^i}\, i\, t^{(i-1)} \tag{29}$$

Due to the nonlinearity of the agglomeration kernel $\beta_0(x_w)$, an exact analytical solution of (29) is impossible, but a numerical solution is straight-forward.
Differentiating (29) with respect to t and inserting the liquid mass balance (4) gives an explicit expression for R_w as a function of $a_1, \ldots, a_{n_p}, t_f, t$:

$$R_w = 10^{-8} \frac{M_{total}}{\beta_0'(x_w)} \sum_{i=2}^{n_p} \frac{a_i}{t_f^i}\, i\,(i-1)\, t^{(i-2)} \tag{30}$$

Another differentiation of (29) finally yields an expression for $\dot{R}_w$ as a function of $a_1, \ldots, a_{n_p}, t_f, t$:

$$\dot{R}_w = 10^{-8} \frac{M_{total}}{\beta_0'(x_w)} \sum_{i=3}^{n_p} \frac{a_i}{t_f^i}\, i\,(i-1)\,(i-2)\, t^{(i-3)} - \frac{\beta_0''(x_w)}{\beta_0'(x_w)} \frac{R_w^2}{M_{total}} \tag{31}$$

Using the described parametrization converts the dynamic optimization problem (23), (24) into the following static optimization problem whose solution does not involve any underlying solution of differential equations:

$$\underset{a_1,\ldots,a_{n_p},t_f}{\text{argmin}} \quad \{-w_1\, M_{product}(\tau(t_f)) + w_2\, x_w(t_f) + w_3\, t_f\} \tag{32}$$

subject to

$$0 < R_w < R_{w,max}, \quad -\dot{R}_{w,max} < \dot{R}_w < \dot{R}_{max}$$
$$\text{equations (27), (28), (29), (30), (31)} \tag{33}$$

The optimization problem is solved numerically by fmincon in Matlab (see Figure 6). It is assumed that the binder spray rate is initially equal to zero. The numerical result can be interpreted as follows: The optimizer aims at reaching the value of τ that is connected to the maximum value of $M_{product}$. This can either be achieved in a slow but binder saving manner, or in a fast way while consuming a higher amount of binder. The ratio between the weighting coefficients w_2 and w_3 determines, if the fast or the slow strategy is used. A large value of w_3 puts emphasis on the production time and results in the fast solution and a higher binder consumption.

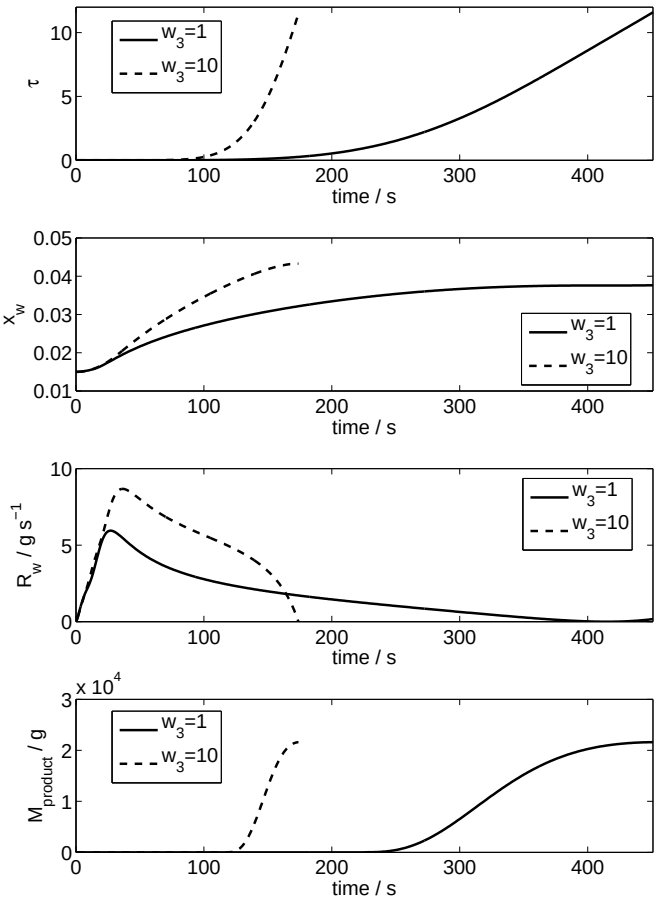

Fig. 6. Optimized feeding strategy for $w_1 = 1$, $w_2 = 4$, $w_3 = 1$ or $w_3 = 10$; $n_p = 9$ is used to parametrize τ.

REFERENCES

A. Bück, G. Klaunick, J. Kumar, Peglow M., and E. Tsotsas. Numerical simulation of particulate processes for control and estimation by spectral methods. *AIChE Journal (in press, available online)*, 2011. doi: 10.1002/aic.12757.

T. Glaser, C. Sanders, F. Wang, I. Cameron, J. Litster, J. Poon, R. Ramachandrian, C. Immanuel, and F. Doyle. Model predictive control of continuous drum granulation. *Journal of Process Control*, 19:615–622, 2009.

P. Holmes, J.L. Lumley, and G. Berkooz. *Turbulence, Coherent Structures, Dynamical Systems and Symmetry.* Cambridge University Press, 1998.

M.J. Hounslow, R.L. Ryall, and V.R. Marshall. A discretized population balance for nucleation, growth and aggregation. *AIChE Journal*, 34:1821–1832, 1988.

M. Krasnyk, M. Mangold, S. Ganesan, and L. Tobiska. Reduction of a crystallizer model with internal and external coordinates by proper orthogonal decomposition. *Chemical Engineering Science*, 70:77–86, 2012.

K. Kunisch and S. Volkwein. Galerkin proper orthogonal decomposition methods for a general equation in fluid dynamics. *SIAM Journal on Numerical Analysis*, 40: 492–515, 2003.

J.D. Litster, D.J. Smit, and M.J. Hounslow. Adjustable discretized population balance for growth and aggregation. *AIChE Journal*, 41:591–603, 1995.

D.L. Marchisio, R.D. Vigil, and R.O. Fox. Implementation of the quadrature method of moments in CFD codes for aggregation-breakage problems. *Chemical Engineering Science*, 58:3337–3351, 2003.

H.M. Park and D.H. Cho. The use of the karhunenloève decomposition for the modeling of distributed parameter systems. *Chemical Engineering Science*, 51: 81–98, 1996.

D. Ramkrishna. *Population balances: theory and applications to particulate systems in engineering.* Academic Press, 2000.

L. Sirovich. Turbulence and the dynamics of coherentstructures. Part 1: coherent structures. *Quarterly of Applied Mathematics*, 45:561–571, 1987.

F.Y. Wang, X.Y. Ge, N. Balliu, and I.T. Cameron. Optimal control and operation of drum granulation processes. *Chemical Engineering Science*, 61:257–267, 2006.